



HAL
open science

Numerical simulation of the DLR-F4 wing/body configuration with wall functions

Eric Goncalvès da Silva, Robert Houdeville

► **To cite this version:**

Eric Goncalvès da Silva, Robert Houdeville. Numerical simulation of the DLR-F4 wing/body configuration with wall functions. ASME 2002 Joint U.S.-European Fluids Engineering Division Conference, Jul 2002, Québec, Canada. pp.1267-1274, 10.1115/FEDSM2002-31097. hal-00217714

HAL Id: hal-00217714

<https://hal.science/hal-00217714>

Submitted on 18 Dec 2018

HAL is a multi-disciplinary open access archive for the deposit and dissemination of scientific research documents, whether they are published or not. The documents may come from teaching and research institutions in France or abroad, or from public or private research centers.

L'archive ouverte pluridisciplinaire **HAL**, est destinée au dépôt et à la diffusion de documents scientifiques de niveau recherche, publiés ou non, émanant des établissements d'enseignement et de recherche français ou étrangers, des laboratoires publics ou privés.

NUMERICAL SIMULATION OF THE DLR-F4 WING/BODY CONFIGURATION WITH WALL FUNCTIONS

Eric Goncalves*

SINUMEF Laboratory - ENSAM
151 bd de l'Hopital
75013 PARIS
FRANCE

Email: Eric.Goncalves@paris.ensam.fr

Robert Houdeville

ONERA-TOULOUSE
Aerodynamics and Energetics Modelling Department
2 avenue Belin - BP 4025
31055 TOULOUSE cedex 4
FRANCE

Email: Robert.Houdeville@oncert.fr

ABSTRACT

This paper deals with the three-dimensional RANS computations of the transonic flow around the DLR-F4 wing-body configuration with a wall law approach. A study of the behaviour of different transport-equation turbulence models is given with comparisons to experimental data. The structure of the three-dimensional flow separation predicted by the computations is described and its topological coherence is checked. Moreover, to drastically reduce the CPU cost, a computation with a multigrid method coupled to wall functions has been tested.

NOMENCLATURE

x, y, z local wall frame (boundary layer).
 U_τ friction velocity.
 C_p pressure coefficient.
 C_f shear stress coefficient.
 P_k turbulent kinetic energy production.
 M_∞ infinite Mach number.
 Re_c Reynolds number based on the mean chord.
 T_i stagnation temperature.
 k turbulent kinetic energy.
 u, v, w velocity components in the local wall frame.
 α angle of attack.
 κ von Karman constant.

ω specific dissipation.
 μ, μ_t molecular and eddy viscosity.
 ρ density.
 w wall value.
 $+$ wall scale.
 1 adjacent cell with respect to the wall.

INTRODUCTION

During the last decade, considerable progress has been made in the development and validation of numerical simulation solvers for complex aerodynamic applications. Today, advanced numerical tools are intensively used in the design process of aerospace components which involve three-dimensional turbulent flows with separation. However, CFD codes still suffer from deficiencies in representativity of computations with respect to the physics, from the lack of accuracy and robustness and from large CPU costs. Indeed, despite the computers growing capacity, the resolution of the RANS equations coupled with a transport-equation turbulence model, integrated down to the wall, for a complete aircraft configuration remains difficult and expensive.

A possibility to avoid the full Navier-Stokes resolution is the use of wall functions as boundary conditions. Thanks to the robustness improvement, the quality of results in two-dimensional separated flows and the CPU cost saving, the wall law approach

* Address all correspondence to this author.

is a promising method (Viegas, 1985; Mohammadi, 1997). However, the existence of a law of the wall for three-dimensional flows is still an open issue. Olcmen (1992) has investigated the possible existence of a universal velocity profile in three-dimensional boundary layers and has concluded that there is not strong evidence for such a 3D turbulent boundary layer velocity profile, neither for the streamwise component nor for the transversal component. In the numerical study of the flow around an ellipsoid, Tsai and Withney (1999) used a logarithmic law for the streamwise direction but changed the value of the constant to obtain a good agreement with the experimental data. In (Goncalves, 2001), the existence of a classical log law for the streamwise velocity component is assumed and excellent results are obtained for the case of the infinite swept wing.

In the present study, the same wall law approach is used to investigate the 3D flow around a wing-body configuration and to compare the behaviour of four popular turbulence models. This configuration has been a European test-case to validate CFD codes and turbulence modelling. It was computed by LeBalleur (1997) using a defect-formulation theory and a 3D thin-layer approach. RANS computations have been performed with the Baldwin-Lomax model (Elsholz, 1997), the Granville algebraic model, the one-equation Wolstein model and the Chen-Patel two-layer model (Tourrette, 1996) and also with an improved $k-\omega$ model (Kroll, 2000). Regarding the shock location, algebraic models can not give predictions with an acceptable level of accuracy. At least a transport-equation model, which takes into consideration history effects, is required to accurately model 3D flow phenomena.

NUMERICAL METHODS

The RANS solver

A code solving the uncoupled RANS/turbulent systems for multi-domain structured meshes is used in the present study. This solver is based on a cell-centered finite volume discretization. For the mean flow, the space-centered Jameson scheme (1981) is used which is stabilized by a scalar artificial dissipation consisting in a blend of 2nd and 4th differences. For the transport equations, a second order upwind Roe scheme (1981) is used to lead to a more robust method.

The time integration procedure is decomposed into 2 steps. The explicit step consists in a four-stage Runge-Kutta algorithm and the implicit step is based on a spectral radius residual smoothing technique, initially proposed by Lerat (1982) and adapted by Jameson (1985) to the Runge-Kutta schemes. More details about the code can be found in (Vuillot, 1993; Liamis, 1994; Couaillier, 1999).

For steady state computations, convergence acceleration is

obtained using a local time step and the classical FAS multigrid method proposed by Jameson (1985, 1991). The turbulent equations are only solved on the fine grid and the computed eddy viscosity μ_t is transferred to the coarse grids.

Various two-equation turbulence models are used in the present study : the Smith (1994) $k-l$ model, the Wilcox (1988) $k-\omega$ model, the Menter (1993, 1994) SST $k-\omega$ model and also the one-equation Spalart-Allmaras (1992) model.

As the discretization scheme does not insure the positivity of the turbulent conservative variables, limiters are used to avoid negative k or ε values. These limiters are set equal to the corresponding imposed boundary values in the far field.

Wall law approach

At the wall, a no-slip condition is used coupled to a wall law treatment. It consists in imposing the diffusive flux densities, required for the integration process, in adjacent cells to a wall. The shear stress τ and the heat flux q are obtained from an analytical velocity profile

$$\begin{aligned} \bar{u}^+ &= y^+ & \text{if } y^+ < 11.13 \\ \bar{u}^+ &= \frac{1}{\kappa} \ln y^+ + 5.25 & \text{if } y^+ > 11.13 \\ \bar{u}^+ &= \bar{u}/U_\tau & ; \quad y^+ = \frac{y/U_\tau}{\nu_w} \end{aligned} \quad (1)$$

and from the integration of the total enthalpy equation, in which the convection is neglected

$$u\tau_{xy} - q_y = -q_w \quad (2)$$

where x and y denote here the longitudinal and normal direction with respect to the wall.

In equation (1), \bar{u} represents the van Driest (1951, 1957) transformed velocity for compressible flows

$$\bar{u} = \int_0^u \sqrt{\frac{\rho}{\rho_w}} du \quad (3)$$

For an adiabatic wall, integration of equations (2) and (3) gives

$$T_w - T = A \frac{u^2}{2} \quad ; \quad A = \frac{\mu + \mu_t}{C_p \left(\frac{\mu}{P_r} + \frac{\mu_t}{P_{r_t}} \right)} \quad (4)$$

$$\bar{u} = \frac{1}{\sqrt{B}} \arcsin(\sqrt{B}u) \quad ; \quad B = \frac{A}{2T_w} \quad (5)$$

The wall law treatment is now straightforward. Knowing u from the Navier-Stokes solution, relationships (4) and (5) give \bar{u} . The shear stress value is obtained from (1) and is assumed constant in the wall normal direction. To compute boundary layer separation, the wall law is expressed in a reference frame defined by the velocity direction in adjacent cells to a wall. Such a treatment is not in contradiction with the fact that the log law does not exist in separated regions. Actually, in these regions, τ_w remains small and therefore y^+ is small, leading to the use of the linear part of the velocity profile. This is equivalent to computing the velocity gradient over two points instead of three for the ordinary cells.

For three-dimensional boundary layers, the existence of a wall law is assumed valid for the streamwise velocity component. Moreover, in adjacent cells to a wall, the velocity is supposed colinear to the wall friction direction. This is the only assumption made regarding the transversal velocity component.

When using the wall law approach with the multigrid algorithm, the wall law boundary condition is applied on the fine grid and the classical no-slip condition is applied on the coarse grids.

As concerns the transport equations of the turbulence models, k is set to 0 at the wall and its production is imposed according to the formulation proposed by Viegas and Rubesin (1983, 1985) where the thickness of the viscous sub-layer y_v^+ is assumed constant

$$(P_k)_1 = \frac{\tau_w^{3/2}}{2\kappa y_1 \sqrt{\rho_w}} \ln \frac{2y_1}{y_v} \quad (6)$$

For the two-equation models, the second variable is deduced from an analytical relation and is imposed in adjacent cells to a wall. The characteristic length scale of the Chen model (1988) is used for the specific dissipation ω and a classical linear law for the length l .

For the one-equation Spalart-Allmaras model, the transported quantity is imposed in adjacent cells to a wall by using the closure relations of the model, the velocity profile and a mixing-length formulation for the eddy viscosity.

More details concerning the wall law approach are given in reference (Goncalves, 2001).

COMPARISON TO EXPERIMENTS

Experimental conditions

The DLR-F4 wing-body configuration has been studied experimentally in three different European wind tunnels (Redeker *et al.*, 1987). The model is representative of a realistic transport-aircraft configuration (1,17m span and 1.19m body length) with

a high aspect ratio transonic wing and an Airbus-type fuselage. The test case is defined as follows : $M_\infty = 0.75$, $\alpha = 0.93^\circ$, $T_i = 300K$, and $Re_c = 3$ millions (based on the aerodynamic mean chord).

For the computations, the flow is assumed to be fully turbulent.

Meshes

The fine mesh used is a single block C-O produced at EADS which defines half of the wing-body configuration. It contains 1129499 nodes, 257 nodes in the main direction, 89 in the normal direction of the wing and 49 in the spanwise direction along the wing. The outer boundaries are fixed at approximately 4 fuselage-lengths (FL) upstream, one FL below and above the configuration and 3 FL downstream. In the spanwise direction, the mesh covers one additional FL.

For computations with wall functions, we used two coarse grids obtained from the fine one by removing planes adjacent to the wing and to the fuselage. The first one contains $257 \times 85 \times 48$ nodes and the y^+ values, at the center of the first cells, vary between 1 and 30 on the wing and between 30 and 80 on the fuselage. The second one contains $257 \times 75 \times 48$ nodes and the y^+ values on the wing are about ten times higher than the corresponding values for the first coarse mesh.

The mesh influence, not discussed here, has been studied by inspecting the shock location and the deviation angle β_0 between the wall friction and the velocity at the boundary layer edge. The best results are obtained with the finest coarse mesh which is chosen for all the computations presented in the following. With the coarser mesh, the assumption that the flow direction is constant in the first cell is no longer valid and leads to a large under-estimation of the β_0 angle in the shock region and near the trailing edge.

In order to use the multigrid method with wall functions, another $257 \times 77 \times 47$ coarse grid has been built from the fine mesh. Convergence problems occur with the multigrid algorithm when a computation is done with the fine mesh.

Convergence and CPU time

In figure 1 is plotted the evolution of residuals for computations with the fine mesh (on the top), wall functions (on the middle) and wall functions with two grids level (on the bottom). The three computations have been carried out with the $k-l$ model. The computation with the fine mesh can not be performed with the implicit residual smoothing while this method can be used for all computations with the wall law approach. With the multigrid method and wall functions, a steady converged result can be obtained with only 800 iterations.

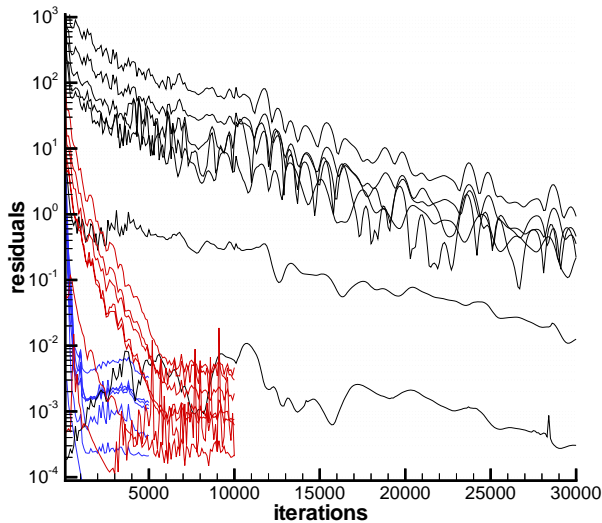


Figure 1. CONVERGENCE HISTORY

The CFL number and the CPU time per iteration are given in table 1 for the same three computations and the one-grid computation with the coarse mesh $257 \times 77 \times 47$.

	CFL number	CPU/iteration
$257 \times 89 \times 49$ - 1 grid level	0.5	2.5s
$257 \times 85 \times 48$ - 1 grid level	3	3.2s
$257 \times 77 \times 47$ - 1 grid level	4	2.91s
$257 \times 77 \times 47$ - 2 grids level	8	4.25s

Table 1. CFL NUMBER AND CPU TIME

The CPU time increasing between the one-grid computations with or without wall functions is due to the use of the implicit step. The wall law approach allows clearly to improve the robustness.

Results

The values of the aerodynamic coefficients of the complete configuration are reported in table 2, for each turbulence model.

	LIFT	DRAG
experiment	0.602	0.0352
$k-l$ (fine mesh without wall functions)	0.651	0.0319
$k-l$	0.638	0.0303
$k-\omega$	0.67	0.0306
$k-\omega$ SST	0.571	0.0261
Spalart-Allmaras	0.61	0.0283

Table 2. LIFT AND DRAG COEFFICIENTS

The best lift coefficient is obtained with the Spalart-Allmaras model. The drag coefficient is underestimated for all computations. The use of a wall law approach, with the Smith model, allows to obtain a lift coefficient closer to the experimental value but the drag coefficient is a little reduced with respect to the fine mesh computation.

The pressure coefficient distribution is shown in figure 2, for three spanwise sections on the wing. The pressure level near the leading edge, on the suction side, is underestimated by all computations. At the closest section to the body, $y/b = 0.185$, the best result is obtained with the $k-l$ model. The Spalart-Allmaras and Menter SST models predict a large and unrealistic separation at the trailing edge.

At the other sections, the shock location is well predicted with the Spalart-Allmaras model and a little downstream with the Smith model. As observed for two-dimensional computations, the Wilcox model predicts a shock location far away from the experimental data and the SST Menter model at an upstream location.

The evolution of the skin friction coefficient in the streamwise direction, on the suction side, is presented in figure 3. There are no experimental values available, only an oil flow picture which does not show any shock-induced separation, which is well predicted by all computations. The SST Menter model gives the lowest skin friction levels. Near the wing root, the Spalart-Allmaras model is close to the Menter model.

The evolution of the deviation angle β_0 , on the suction side, is considered in figure 4. There is a clearly pronounced peak at the shock location, the wall flow being deviated towards the wing tip. The SST model predicts large values of the deviation in the shock region and at the trailing edge. At the closest section to the body, as noticed on the pressure distribution, the Spalart-Allmaras and Menter models predict a large separation.

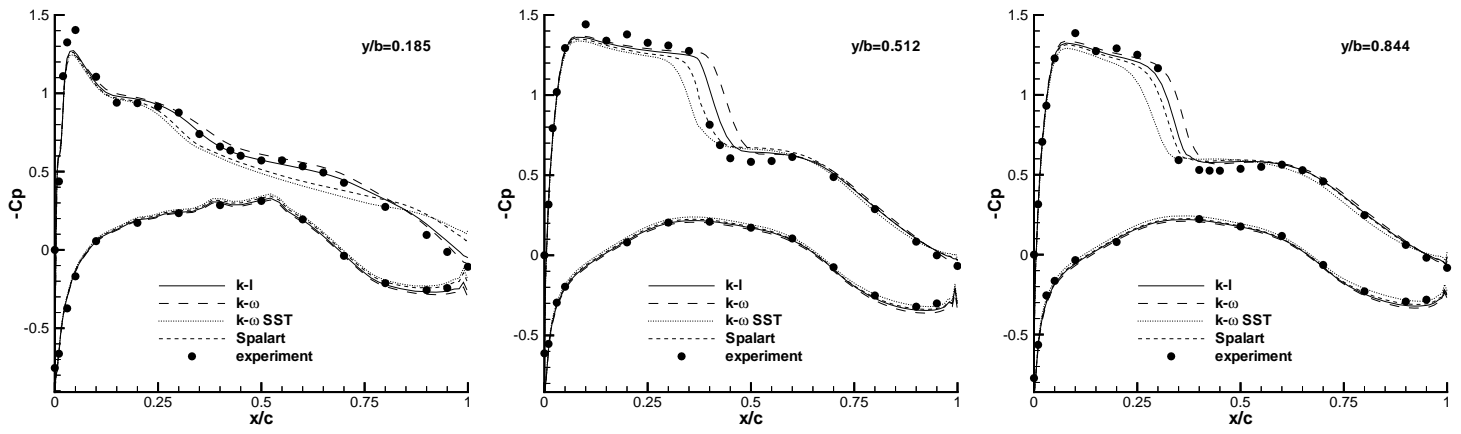


Figure 2. PRESSURE COEFFICIENT

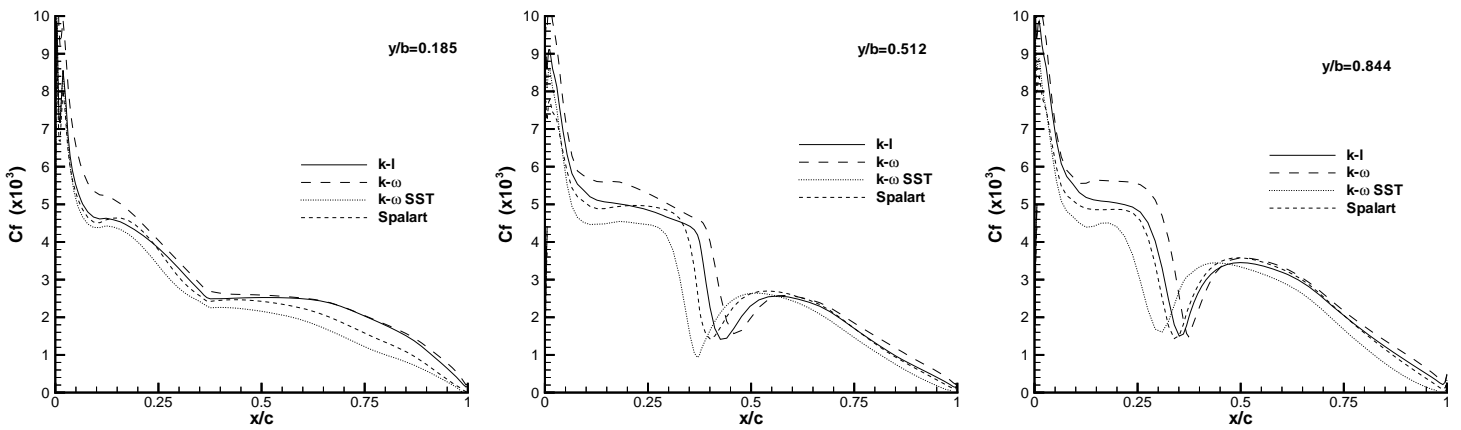


Figure 3. SKIN FRICTION COEFFICIENT

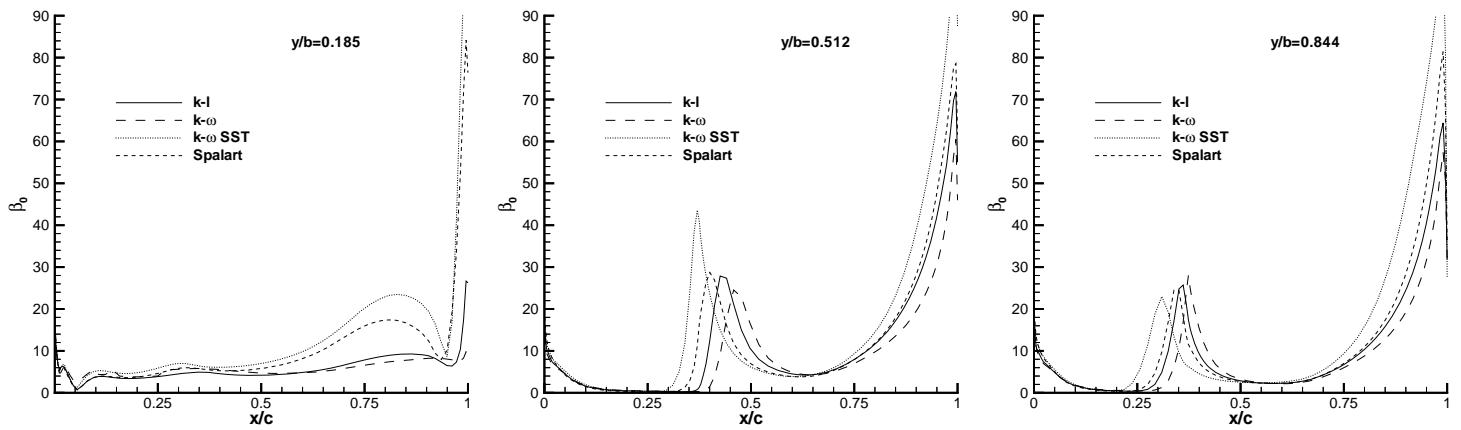


Figure 4. DEVIATION ANGLE β_0

The skin friction lines over the half configuration are plotted in figure 5, computed with the Smith model. A horse-shoe vortex footprint around the wing root can be seen and also a vortical structure footprint at the trailing edge, near the root of the wing. The experimental oil flow picture also shows a vortex-like structure at the wing root but there is no flow visualization for the fuselage.

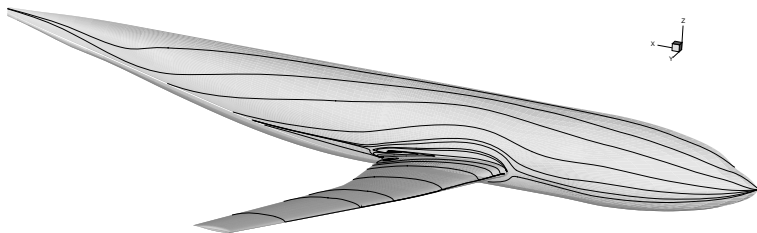


Figure 5. SKIN FRICTION LINES - SMITH MODEL

An enlargement of the wing/body junction, at the leading edge of the wing, is presented in figure 6. We can well observe the horse-shoe vortex around the root, the saddle point on the fuselage and the stagnation point on the wing. Such a separation has been evidenced by Furlano (2001) for 3D computations of an airfoil between walls, using the $k-l$ Smith model. In these results, the stagnation point is located on the fuselage. In the present case, it is certainly the sweep angle effect which moves the stagnation point on the wing. It can be noted that all turbulence models predict the same flow topology.

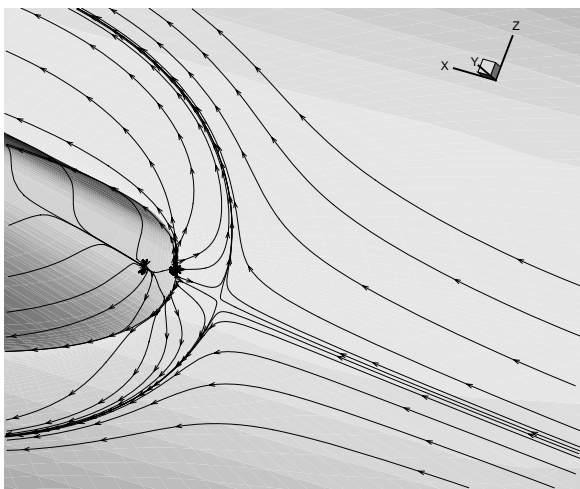


Figure 6. DETAIL OF THE LEADING EDGE - SMITH MODEL

The horse-shoe vortex feeds a vortical structure, called tornado vortex. The footprint of this vortex on the wing and the body is a focus, interpreted as a rolling up of the separation surface. This structure is generated by the interaction between the boundary layers of the wing and the fuselage (Delery, 1992). A detail of the wing/body junction, at the trailing edge of the wing, is presented in figure 7, computed with the Smith model. The tornado vortex with the two foci are clearly evidenced. We note a third focus on the fuselage, interpreted as an unrolling of the flow, which feeds the focus on the body, already fed by the horse-shoe vortex. This third focus allows to preserve the volume of the stagnation flow of the vortical structure. Moreover, when using a very large close-up view of the trailing edge vicinity, it has been possible to identify a second saddle point and a node near the third focus, on the wing/body junction. Downstream of the tornado vortex, on the fuselage, is located a third saddle point which ends the horse-shoe vortex surrounding the wing/body junction. Finally, we have three foci, three saddle points and two nodes (the stagnation point being equivalent to a node). To check the coherence of the three-dimensional separation, we use the following relation based on the critical-point theory and only valid for an isolated obstacle (Delery, 1992) :

$$\Sigma(\text{nodes and foci}) - \Sigma(\text{saddle points}) = 2 \quad (7)$$

This relation is well respected but one should be careful, the identification of all critical points could be difficult.

When compared to the result obtained with the Smith model, the vortical structure predicted by the Wilcox model (figure 8) and the Spalart-Allmaras model (figure 10) presents a similar topology. This structure is a little less extended for the first model and largely overestimated by the second one. The big vortical structure with five foci predicted by the SST Menter model (figure 9) is completely unphysical. This is not so surprising, the SST correction being based on two-dimensional considerations.

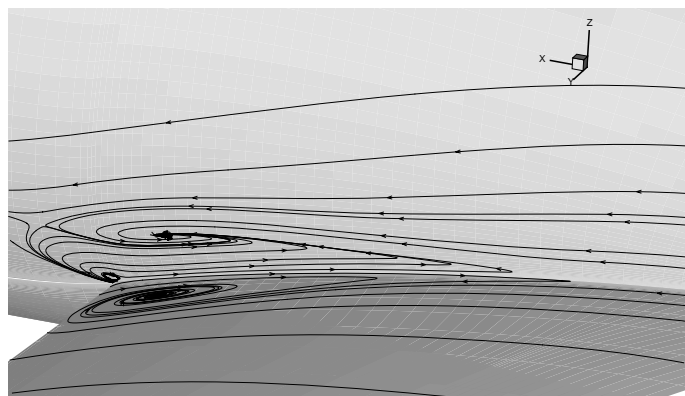


Figure 7. DETAIL OF THE TRAILING EDGE - SMITH MODEL

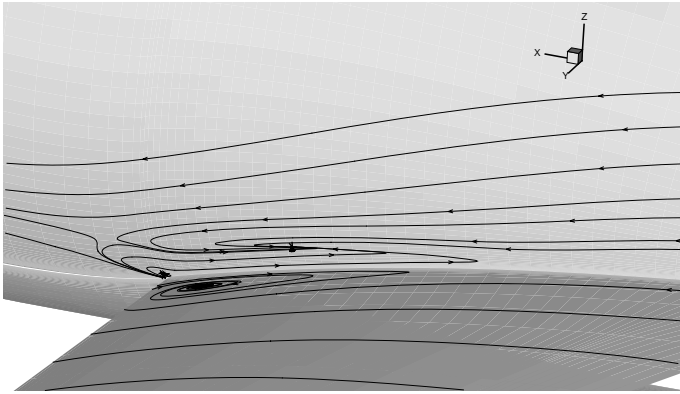


Figure 8. DETAIL OF THE TRAILING EDGE - WILCOX MODEL

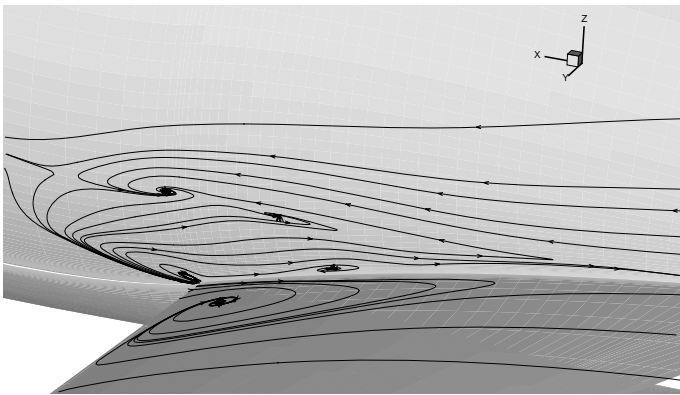


Figure 9. DETAIL OF THE TRAILING EDGE - MENTER SST MODEL

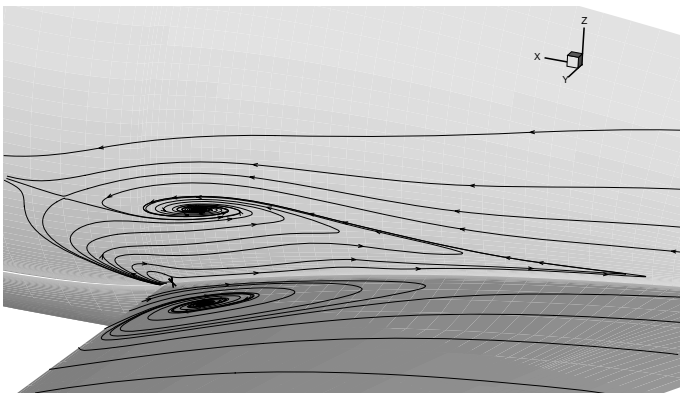


Figure 10. DETAIL OF THE TRAILING EDGE - SPALART-ALLMARAS MODEL

In figure 11 is plotted the vortical structure obtained without wall functions using the fine mesh and the Smith model. The topology of the separation is similar but the rolling up focus on the fuselage is moved toward the leading edge.

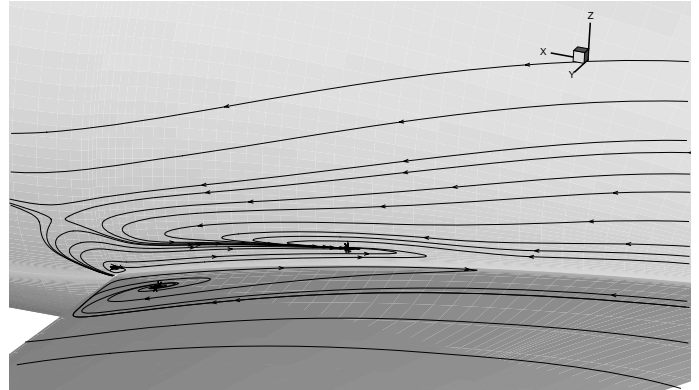


Figure 11. DETAIL OF THE TRAILING EDGE - SMITH MODEL - FINE MESH

CONCLUSION

This study shows the capability of a wall law approach to correctly predict the three-dimensional flow around a wing/body configuration and allows to compare the behaviour of four popular turbulence models. When comparing the pressure coefficient distribution, the Smith and the Spalart-Allmaras models provide the best results. Yet, near the wing root, the Spalart-Allmaras model predicts a large and unrealistic separation. As observed for two-dimensional computations over airfoils, the Wilcox model predicts a shock location far away from the experimental data and the SST Menter model at an upstream location.

As concerns the 3D separated flow generated on the wing-body junction, all models predict a coherent topological structure, except the SST Menter model which yields an unphysical vortical structure. This is certainly due to the SST correction based on the Bradshaw hypothesis, established for two-dimensional turbulent boundary layers.

Not only does the wall law approach allow to obtain accurate results, it also offers large CPU cost saving when coupled with a multigrid technique. Using such tools make unsteady three-dimensional computations at hand.

ACKNOWLEDGMENT

This work has been carried out at the Department Models for Aerodynamic and Energetics of ONERA-Toulouse.

REFERENCES

- Chen, H.C. and Patel, V.C., *Near-Wall Turbulence Models for Complex Flows Including Separation*, AIAA Journal, vol. 26(6), pp.641-648, 1985.
- Couaillier, V., *Numerical Simulation of Separated Turbulent Flows Based on the Solution of RANS/Low Reynolds Two-Equation Model*, AIAA 99-0154, 37th Aerospace Sciences Meeting & Exhibit, Reno, Nevada, January 11-14 1999.
- Delery, J.M., *Physics of vortical flows*, Journal of Aircraft, vol.29(5), pp.856-876, 1992.
- Elsholtz, E., John, D., *3D Navier-Stokes mesh generation and analysis of viscous flow solution around the DLR-F4 wing-body configuration*, ECARP - Validation of CFD Codes and Assessment of Turbulence Models. Notes on Numerical Fluid Mechanics, Vol. 58, pp.69-80, Vieweg 1997.
- Furlano, F., Coustols, E., Plot, S., Rouzaud, O., *Steady and unsteady computations of flows close to airfoil buffeting: validation of turbulence models*, TSFP, Stockholm, Sweden, June 27-29, 2001.
- Goncalves, E., and Houdeville, R., *Reassessment of the wall functions approach for RANS computations*, Aerospace Science and Technology, vol. 5, pp.1-14, 2001.
- Jameson, A., Schmidt, W., Turkel, E., *Numerical simulation of the Euler equations by finite volume method using Runge-Kutta time stepping schemes*, AIAA paper 81-1259, 1981.
- Jameson, A., *Multigrid Algorithms for Compressible Flow Calculations*, Lecture Notes in Mathematics n° 1228, Springer-Verlag, 1985.
- Jameson, A., *Time Dependent Calculations Using Multigrid with Applications to Unsteady Flows past Airfoils and Wings*, AIAA paper 91-1259, 10th Computational Fluid Dynamics Conference, Honolulu, Hawaii, 1991.
- Kroll, N., Rossow, C.C., Becker, K., Thiele, F., *The MEGAFLOW project*, Aerospace Science and Technology, vol. 4, pp.223-237, 2000.
- Le Balleur, J.C., Girodroux-Lavigne, P., and Neron, M., *Viscous-Inviscid Interaction Methods in 2D/3D-Steady/Unsteady-Problems*. ECARP - Validation of CFD Codes and Assessment of Turbulence Models. Notes on Numerical Fluid Mechanics, Vol. 58, pp.197-222, Vieweg 1997.
- Lerat, A., Sides, J., and Daru, V., *An Implicit Finite-Volume Method for Solving the Euler Equations*, Lecture Notes in Physics, Springer-Verlag, 1982.
- Liamis, N., and Couaillier, V., *Unsteady Euler and Navier-Stokes Flow Simulations with an Implicit Runge-Kutta Method*, 2nd European Comput. Fluid Dynamics Conference, Stuttgart, published by John Wiley & sons, 1994.
- Menter, F.R., *Zonal two equation $k - \omega$ turbulence models for aerodynamic flows*, AIAA 93-2906, 24th Fluid Dynamics Conference, Orlando, Florida, July 6-9 1993.
- Menter, F.R., *Two-equation eddy-viscosity turbulence models for engineering applications*, AIAA Journal, vol. 32(8), pp.1598-1605, 1994.
- Mohammadi, B., and Pironneau, O., *Unsteady separated turbulent flows computation with wall-laws and $k - \epsilon$ model*, Computational Methods in Applied Mechanical Engineering., 148, pp.393-405, 1997.
- Olcmen, M.S., and Simpson, R.L., *Perspective : on the near wall similarity of three-dimensional turbulent boundary layers*, Journal of Fluids Engineering, vol. 114, pp.487-495, December 1992.
- Redeker, G., Muller, R., Ashill, R., Elsenaar, P.R., Schmitt, V., *Experiments on the DLR-F4 wing-body configuration in several European windtunnels*, AGARD-FDP-Symposium, Sept.28-Oct.1, Naples, Italy, 1987.
- Roe, P.L., *Approximate Riemann solvers, parameters vectors, and difference schemes*, Journal of Computational Physics, vol. 43, pp.357-372, 1981.
- Smith, B.R., *A Near Wall Model for the $k - l$ Two Equation Turbulence Model*, AIAA 94-2386, 25th Fluid Dynamics Conference, Colorado Springs, Colorado, June 20-23 1994.
- Spalart, P.R., and Allmaras, S.R., *A one-equation turbulence model for aerodynamic flows*, AIAA 92-0439, 30th Aerospace Sciences Meeting, Reno, Nevada, January 6-9 1992.
- Tourrette, L., *Assessment of turbulence models for the transonic flow around the DLR-F4 wing/body configuration*, AIAA 96-2034, 27th Fluid Dynamics Conference, New Orleans, Louisiana, June 17-20 1996.
- Tsai, C.Y., and Whitney, A.K., *Numerical study of three-dimensional flow separation for a 6:1 ellipsoid*, AIAA 99-0172, 37th Aerospace Sciences Meeting & Exhibit, Reno, Nevada, January 11-14, 1999.
- van Driest, E.R., *Turbulent Boundary Layer in Compressible Fluids*, J. Aeronaut. Sci., vol. 18, pp.145-160, 1951.
- van Driest, E.R., *On Turbulent Flow Near a Wall*, J. Aeronaut. Sci., vol. 23, pp.1007-1011, 1957.
- Viegas, J.R., and Rubesin, M.W., *Wall-Function Boundary Conditions in the Solution of The Navier-Stokes Equations for Complex Compressible Flows*, AIAA 83-1694, 16th Fluid and Plasma Dynamics Conference, Danver, Massachusetts, July 12-14 1983.
- Viegas, J.R., Rubesin, M.W., and Horstman, C.C., *On the Use of Wall Functions as Boundary Conditions for Two-Dimensional Separated Compressible Flows*, AIAA 85-0180, 23rd Aerospace Sciences Meeting, Reno, Nevada, January 14-17, 1985.
- Vuillot, A.M., Couaillier, V., and Liamis, N., *3D Turbomachinery Euler and Navier-Stokes Calculations with Multidomain Cell-Centered Approach*, AIAA Paper 93-2576, 1993.
- Wilcox, D.C., *Reassessment of the scale-determining equation for advanced turbulence models*, AIAA Journal, vol. 26(11), pp.1299-1310, 1988.